



Contents lists available at ScienceDirect

Experimental Eye Research

journal homepage: www.elsevier.com/locate/yexer

Quantitative and regional measurement of retinal blood flow in rats using N-isopropyl-p-[¹⁴C]-iodoamphetamine ([¹⁴C]-IMP)

Mylène Pouliot^{a,b}, Micheline C. Deschênes^{a,c,d}, Simon Héту^{a,b}, Sylvain Chemtob^e,
Mark R. Lesk^{c,d}, Réjean Couture^b, Elvire Vaucher^{a,*}

^a School of Optometry, University of Montreal, C.P. 6128, succursale Centre-Ville, Montréal, QC H3C 3J7, Canada¹

^b Department of Physiology, University of Montreal, C.P. 6128, succursale Centre-Ville, Montréal, QC H3C 3J7, Canada²

^c Department of Ophthalmology, University of Montreal, C.P. 6128, succursale Centre-Ville, Montréal, QC H3C 3J7, Canada³

^d Research Centre Guy-Bernier, University of Montreal, Maisonneuve-Rosemont Hospital, 5415 boul. L'Assomption, Montréal, QC H1T 2M4, Canada⁴

^e Departments of Pediatrics, Ophthalmology and Pharmacology, Research Centre of Sainte-Justine Hospital, 3175 Côte Sainte-Catherine, Montréal, Québec H3T 1C5, Canada⁵

ARTICLE INFO

Article history:

Received 9 June 2009

Accepted in revised form 12 August 2009

Available online xxx

Keywords:

blood flow

retina

brain

autoradiography

hypercapnia

iodoamphetamine

microcirculation

imaging

ABSTRACT

Quantitative and regional measurement of retinal blood flow in rodents is of prime interest for the investigation of regulatory mechanisms of ocular circulation in physiological and pathological conditions. In this study, a quantitative autoradiographic method using N-isopropyl-p-¹⁴C-iodoamphetamine ([¹⁴C]-IMP), a diffusible radioactive tracer, was evaluated for its ability to detect changes in retinal blood perfusion during hypercapnia. Findings were compared to cerebral blood flow values measured simultaneously. Hypercapnia was induced in awoken Wistar rats by inhalation of 5% or 8% CO₂ in medical air for 5 min. [¹⁴C]-IMP (100 µCi/kg) was injected in the femoral vein over a 30 s period and the rats were sacrificed 2 min later. Blood flow was calculated from whole-mount retinae and 20 µm thick brain sections in discrete regions of interest by quantitative autoradiography or from digested samples of retina and brain by liquid scintillation counting. Retinal blood flow values measured with quantitative and regional autoradiography were higher in the central (108 ± 20 ml/100 g/min) than in peripheral (84 ± 15 ml/100 g/min) retina. These values were within the same range as cortical blood flow values (97 ± 4 ml/100 g/min). The retinal blood flow values obtained on whole-mount retinae were validated by the sampling method. Hypercapnia significantly increased overall blood flow in the retina (24–53%) with a maximal augmentation in the peripheral region and in the brain (22–142%). The changes were stronger in the brain compared to retina ($p = 0.016$). These results demonstrate that retinal blood flow can be quantified using [¹⁴C]-IMP and compared with cerebral blood flow. This technique is a powerful tool to study how retinal blood flow is regulated in different regions of the rat retina.

© 2009 Elsevier Ltd. All rights reserved.

1. Introduction

Deficit in blood supply in the retina contributes to the development of retinal diseases, such as diabetic retinopathy, age-related macular degeneration and glaucoma (Grunwald et al., 1984; Langham et al., 1991; Atmaca et al., 1996). Rodent models are commonly used to

study the development of these retinal damages and to test potential therapies. However, blood flow dysfunctions in rodents and their cellular and molecular mechanisms remain elusive. This is principally due to a lack of a technical approach which would adequately assess all the specific features of the rodent retinal microcirculation.

Due to its small size, laminar structure, location and apposition to the choroid, the rodent retina is particularly difficult to study. Optically based imaging techniques, including laser Doppler flowmetry (Tsuji-kawa et al., 2000; Yu et al., 2005; Chauhan et al., 2006; Mori et al., 2007), on-line video angiography (Clermont et al., 1994; Kunisaki et al., 1998) or optical coherence tomography (Fujimoto et al., 1995) have a great temporal resolution but a poor spatial and laminar resolution and require a high transparency of the light paths (Glazer, 1988; Duong et al., 2008). Alternatively, quantitative techniques such as the use of systemic radioactive or non-radioactive microspheres (Chemtob et al., 1991; Alm et al., 1997; Wang et al., 2007) and magnetic

Abbreviations: CBF, cerebral blood flow; DLG, dorsolateral geniculate nucleus; IMP, iodoamphetamine; RBF, retinal blood flow.

* Corresponding author. Tel.: +1 514 343 7537; fax: +1 514 343 2382.

E-mail address: elvire.vaucher@umontreal.ca (E. Vaucher).

¹ Tel.: +1 514 343 7537; fax: +1 514 343 2382.

² Tel.: +1 514 343 7060; fax: +1 514 343 2111.

³ Tel.: +1 514 343 7094; fax: +1 514 343 5790.

⁴ Tel.: +1 514 252 3400x4959; fax: +1 514 343 3821.

⁵ Tel.: +1 514 345 4692; fax: +1 514 345 4801.

resonance imaging (Sicard and Duong, 2005; Duong et al., 2008; Li et al., 2008) are performed on anesthetised animal which modifies cardiovascular parameters. The use of radioactive diffusible tracer iodoantipyrine commonly used for the measurement of cerebral blood flow (CBF) (Sakurada et al., 1978; Bryan et al., 1988; Vaucher et al., 1997; Greenberg et al., 1999) has also been tested for quantitative measurement of retinal blood flow by autoradiography in the cat, monkey (Sossi and Anderson, 1983; Quigley et al., 1985) and rat (O'Brien et al., 1997), but post-mortem tracer diffusion limits its spatial resolution (Caprioli and Miller, 1988).

In order to simultaneously provide quantitative and local measurement of discrete changes of the retinal blood flow (RBF) in conscious rats, the autoradiographic technique was adapted in the present study by using the radioactive diffusible tracer N-Isopropyl-p-[¹⁴C]-iodoamphetamine ([¹⁴C]-IMP). This tracer was chosen because it has an insignificant post-mortem diffusion so that tissue perfusion could be quantified in whole-mount retina isolated from the choroid. The principle of blood flow evaluation with [¹⁴C]-IMP is identical to that of micrometric microspheres (Wang et al., 2007) except that this "molecular microsphere" –IMP– is freely diffusible (does not depend on the blood-retinal or blood-brain barrier) and is trapped within the tissue instead of the microvascular space. It is then possible to quantify tissue perfusion at a microvascular level throughout the retina by computerized autoradiography. Moreover, the use of a diffusible tracer avoids inaccuracies of the RBF measurement due to axial streaming, plugging or permeability changes as reported with the classical microsphere technique (Glazer, 1988; Wang et al., 2007). Autoradiography technique is usually performed on 20 µm thick brain sections, whereas the flat mount retina is on average 200 µm thick. In order to validate RBF values measured by autoradiography, samples of the retina were digested and analyzed by liquid scintillation counting (O'Brien et al., 1997). Finally, as hypercapnia is commonly used to test the metabolic vasodilatation, two hypercapnia regimens were used to challenge the sensitivity of this technique to assess RBF changes. In addition, this technique provided the opportunity to simultaneously assess the RBF and CBF, which is an additional advantage to assess the tissue specificity of the responses to diverse physiological stresses.

2. Materials and methods

2.1. Animals

Male Wistar rats ($n = 20$; 200–250 g) purchased from Charles River (St-Constant, Qc, Canada) were used for the measurement of RBF and CBF using [¹⁴C]-IMP by autoradiography or the sampling method. Rats were housed individually and placed in a room at 23 °C with a 12 h light/dark adapted photoperiod, with food and water provided *ad libitum*. All experimental methods and animal care procedures were approved by the local institutional animal care committee, "Comité de Déontologie de l'Expérimentation sur les Animaux" at the University of Montreal, under the auspices of the Canadian Council on Animal Care.

2.2. Surgical procedure

Polyurethane catheters were inserted into the femoral vein (Micro-Renathane, I.D. 0.040", O.D. 0.020", Braintree Scientific, Braintree, MA, USA) and artery (Tygon Micro Bore, I.D. 0.010", O.D. 0.030", Small Parts, Miramar, FL, USA) under 1.5% isoflurane (induction of anesthesia with 3% isoflurane for 5 min). During this procedure, body temperature was monitored with a rectal thermometer and maintained at 37 °C by a heating pad (FHC, Bowdoinham, ME). Both blood pressure and heart rate were monitored from the tail using a non-invasive blood pressure cuff system (BP1000, Kent Scientific Corporation, Torrington, CT, USA). Before and immediately

after the surgery, the topical anesthetic lidocaine hydrochloride 2% (AstraZeneca, Mississauga, Ont, Canada) was applied on the skin incision to minimize pain. Rats were then installed in a hammock and left under minimal restraint over a 2 h period to recover from anesthesia. Body temperature was maintained at 37 °C with a heating lamp and both blood pressure and heart rate were monitored until the initiation of measurement experiment for the retinal perfusion. As well, cardiovascular, chemistry and hematologic parameters were measured with a veterinarian clinical blood gases and electrolytes analyzer (i-STAT[®], HESKA, Fort Collins, CO), from arterial blood samples collected via the arterial catheter. These data were collected immediately prior to the initiation of hypercapnia to confirm the recovery to a normal physiological level.

2.3. Induction of hypercapnia

Hypercapnic conditions were used to modulate RBF and CBF. Awake animals were acclimatized to a gentle flow of medical air (3 L/min; 21% O₂, 79% N₂) provided by a small mask placed on the nose and mouth. Following few minutes of normal air breathing, hypercapnia was induced by inhalation of 5% CO₂ ($n = 4$) or 8% CO₂ ($n = 5$) in medical air. Elevation of CO₂ concentration in inspired air started 5 min prior to the injection of [¹⁴C]-IMP for retinal perfusion measurement and lasted until the animals were sacrificed. Cardiovascular and hematologic parameters were also monitored during hypercapnia induction. Control animals ($n = 9$) inhaled only medical air.

2.4. Principles of the evaluation of retinal tissue perfusion using IMP

To evaluate tissue perfusion in retina with a regional resolution, we chose the diffusible blood flow tracer [¹⁴C]-IMP because of its three essential properties for CBF measurement (Lear et al., 1982). First, [¹⁴C]-IMP has a high extraction at the first pass through the microvasculature, which allows a non-restrictive diffusion from blood to tissue despite the blood-retinal barrier. Second, [¹⁴C]-IMP has a low clearance rate and low post-mortem diffusion (Greenberg et al., 1999; Bryan et al., 1988) due to its high affinity for cerebral tissue. This property avoids the primary limitation to the classical diffusible tracer [¹⁴C]-iodoantipyrine autoradiographic technique (O'Brien et al., 1997) or of the *n*-[¹⁴C]-butanol (Puchowicz et al., 2004), i.e. their time-dependent post-mortem intraparenchymal diffusion, which results in weakening the local tracer spatial gradients in tissues. Third, [¹⁴C]-IMP is chemically and biologically inert for the duration of the measurement period (Greenberg et al., 1999). IMP has been successfully used in small animal research (Lear et al., 1982; Greenberg et al., 1999; Temma et al., 2004) and in humans using Single Photon Emission Computerized Tomography (Lear et al., 1982).

2.5. Procedure for the measurement of retinal and cerebral blood flow

(D,L)-N-Isopropyl-4-[¹⁴C]-iodo(phenyl)amphetamine (100 µCi/kg; PerkinElmer, Boston, MA, USA, custom synthesis) was dissolved in 600 µL of saline (injectable 0.9% NaCl solution) and infused in fully conscious rats over a 30 s period at a constant rate of 1.2 mL/min using an infusion pump (PHD 2000, Harvard Apparatus, Holliston, MA, USA) through the femoral vein. An average of 20–24 arterial blood samples (10 µL) were collected continuously from the beginning of [¹⁴C]-IMP injection to the sacrifice of the animal (2 min) in order to evaluate the arterial contamination curve. Blood samples were digested in 300 µL of solouene (PerkinElmer, Boston, MA, USA) for 2 h at 37 °C. A total of 5 ml of scintillation fluid (Ultimagold, PerkinElmer, Boston, MA, USA) was then added and the radioactivity was counted in a scintillation

counter (LS6500, Beckman Coulter, Mississauga, ON, Canada). The rats were sacrificed by decapitation 2 min after the beginning of the infusion. The eyes and brain were quickly removed within 3 min. A small incision on the superior eyelid was made to indicate the orientation of the eyes and the eyes together with the attached superior eyelid were then harvested. The eyes were immediately excised, the lens removed and the eye cup immersed in a solution of 4% paraformaldehyde for post-fixation. After a 1 h fixation, retinæ were removed from the eye cup, and dissected into four quadrants (superior, inferior, nasal and temporal). The vitreous body was carefully removed from the retinæ using fine paint brush. One retina was processed for the sampling method the other one for autoradiographic analysis.

2.5.1. Sampling method

The whole wet retina was weighed after removal of vitreous body and digested in 500 μL of soluene overnight at 37 °C, then processed for liquid scintillation counting (see above). In addition, 3 retinæ from distinct control animals ($n = 2$) were microdissected (1 mm² strips from each isopter and quadrant), weighed and analyzed by liquid scintillation. The counts were expressed in $\mu\text{Ci/g}$.

2.5.2. Autoradiography

The retina of the opposite eye was whole-mounted on a glass slide with the ganglion cells layer away from the slide. A small incision was made on the retina to indicate the nasal quadrant. The whole-mount retina was then exposed to an X-ray film (Hyperfilm, GE Healthcare Ltd, UK) for 4 days together with a set of [¹⁴C]-standards (ARC, St. Louis, USA). The autoradiograms were analyzed using the computerized image analysis MCID Basic Software (v7.0, Interfocus Imaging, Linton, England).

For the CBF quantification, a piece of the frontal cerebral cortex was dissected, weighed and digested in soluene overnight at 37 °C for liquid scintillation counting, and the remaining brain was frozen in isopentane (–55 °C) for autoradiography. The frozen brain was subsequently sliced in 20 μm thick coronal sections using a cryostat (–22 °C) and exposed on X-ray film for 8 days with [¹⁴C]-standards (Amersham Biosciences, UK). Optimal exposure time for brain and retina was determined from pilot experiments.

2.6. Calculation of retinal and cerebral blood flow

Retinal and cerebral blood flow was evaluated using the principle of indicator-fractionation technique (Lear et al., 1982; Greenberg et al., 1999) using the equations Eq. (1) for sampling method and autoradiographic analysis performed with 20 μm thick sections and Eq.(2) for autoradiographic analysis performed on whole-mount retinæ.

$$F = \left[C_{\text{IMP}}(T) / \int_0^T \text{Ca}(t) \right] \quad (1)$$

$$F = \left[C_{\text{IMP}}(T) \times 10^{-1} / \int_0^T \text{Ca}(t) \right] \quad (2)$$

where F is the blood flow (ml/100 g/min), $C_{\text{IMP}}(T)$ is the radioactivity measured on the autoradiogram or digested tissue ($\mu\text{Ci/g}$) at the time T (min) of sacrifice and $\text{Ca}(t)$ is the arterial concentration of radioactivity measured in the blood samples ($\mu\text{Ci/ml}$). For autoradiographic measurements in the retina, $C_{\text{IMP}}(T)$ was read from circular regions of interest of 0.8 mm² (1 mm diameter) distributed at the 1, 2 and 3 mm isopters away from the center of the optic nerve head in all retinal quadrants (Fig. 1). Since the common

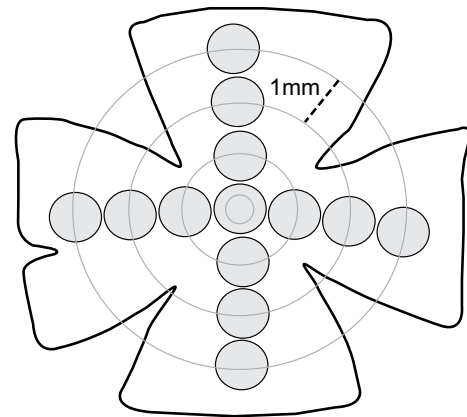


Fig. 1. Schematic representation of a whole-mount retina showing the regions of interest measured. The retina was divided into four quadrants (the notch indicates the nasal quadrant). The radioactivity concentration, $C_{\text{IMP}}(T)$, was measured in a circular region of interest (filled circles, area 0.8 mm²) in the center of the retina (optic nerve head) and in each quadrant at each isopter (light circular lines at 1, 2 and 3 mm away from the center of optic nerve head).

radioactive standards used for autoradiography are calibrated for 20 μm thick sections and the rat retina thickness is $205 \pm 11 \mu\text{m}$ (Duong et al., 2008), the measured [¹⁴C]-IMP concentration values from autoradiograms ($C_{\text{IMP}}(T)$) were uniformly corrected by a factor 10. For the brain, 8 regions of interest (area adjusted to the region size, 2–9 mm²) related to vision or in control areas were selected and analyzed at 3 coronal levels from Bregma: AP + 1.6 mm; cingulate, frontal cortex, striatum; AP –4.5 mm; parietal cortex, hippocampus, dorsolateral geniculate nucleus (DLG); AP –6.3 mm; occipital cortex, superior colliculus.

2.7. Statistical analysis

Non-parametric Mann–Whitney tests were performed to compare both hypercapnic groups with control group and compare 5% CO₂ group with 8% CO₂ group for (1) the physiological parameters, (2) the regional RBF of each isopter, (3) the total RBF in digested tissue and (4) the CBF. For intragroup comparison of regional RBF, non-parametric Mann–Whitney tests were performed to compare isopter 3 mm with optic nerve head and isopter 1 mm. A significance level of $p < 0.05$ was chosen.

3. Results

3.1. Quantitative and regional measurement of retinal blood flow in control animals

Pseudocolor autoradiograms of whole-mount retinæ displayed a gradient of blood flow from the center of the retina to the periphery (Fig. 2, Table 1). The blood flow values were significantly higher in the optic nerve head region ($108 \pm 20 \text{ ml}/100 \text{ g}/\text{min}$) and isopter 1 mm ($112\text{--}120 \text{ ml}/100 \text{ g}/\text{min}$, according to the quadrants examined) than in the isopter 3 mm ($82\text{--}86 \text{ ml}/100 \text{ g}/\text{min}$, according to the quadrants examined, $p < 0.05$, Table 1). The values of blood flow throughout each concentric isopter were homogeneous. To validate the whole-mount measurements, sampling by isopter was performed by soluene digestion of retina samples controlled for their weight. The same center-to-periphery gradient of RBF values was observed with this method (optic nerve head, 138 ± 18 vs. isopter 3 mm, $89 \pm 13 \text{ ml}/100 \text{ g}/\text{min}$, $p = 0.04$, Table 2).

The values of RBF measured using the autoradiographic or sampling methods were within the same range, i.e. 80–120 ml/100

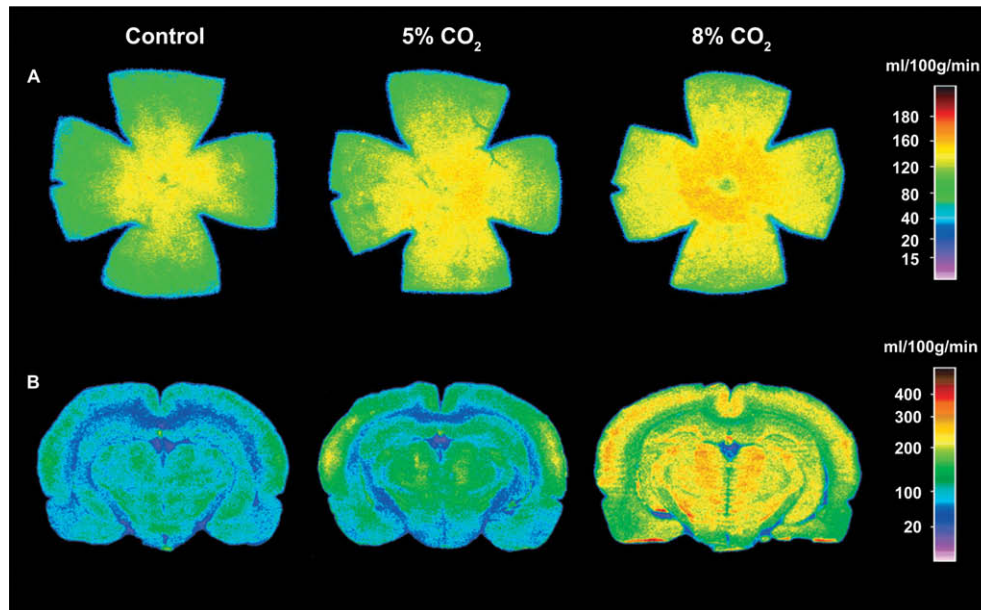


Fig. 2. Representative whole-mount retina (A) and brain (B) autoradiograms displayed in pseudocolor from a control and two hypercapnic rats (5% CO₂ and 8% CO₂). The correspondence between pseudocolor scale and blood flow values (ml/100 g/min) is represented on the right side of the figure. For the retinae as well as for the brains, the tissue concentration of [¹⁴C]-IMP was higher in hypercapnic rats than in control rats, indicating that the blood perfusion was greater. (A) Retinal blood flow was increased in both hypercapnic groups compared to control group. (B) Representative autoradiograms of 20 μm coronal brain sections at the level of the dorsal geniculate nucleus (- 4.6 mm from Bregma). The cerebral blood flow changes induced by hypercapnia varied according to the region examined.

g/min (Fig. 2, Table 1, 2). This equivalence validates the correction factor ($x \times 10^{-1}$) of the measured [¹⁴C]-IMP concentration values from whole-mount retina autoradiograms. However, it has to be considered that the peripheral retina might be slightly thinner than its central part whereas the correction for the retina thickness performed was a constant. This could introduce a slight quantitative bias when comparing central vs. peripheral values but not when comparing counterparts regions from one retina to the other.

Moreover, our quantitative results showed that RBF values were within the same range that the cortical blood flow values, using both methods (80–120 vs. 70–127 ml/100 g/min, respectively, Table 1).

3.2. Physiological parameters

Before the inhalation of CO₂ (pre-hypercapnic values), physiological parameters were not different in the hypercapnic groups than in the control group ($p > 0.05$, Table 3). pCO₂, pO₂ and HCO₃ were significantly increased in the 5% CO₂ group ($p = 0.029$) and 8% CO₂ group ($p = 0.008$). The pH was significantly decreased in the 5% CO₂ group ($p = 0.029$) and 8% CO₂ group ($p = 0.008$) compared to pre-hypercapnic values as commonly found in hypercapnia studies (Dauphin et al., 1991). Body temperature, blood pressure and heart rate were not affected by hypercapnia ($p > 0.05$, Table 3).

3.3. Effects of hypercapnia on retinal and cerebral blood flow

The hypercapnia induced a significant increase in the RBF ranging from 24% to 34% in the 5% CO₂ group and from 31% to 53% in the 8% CO₂ group ($p < 0.05$, Table 1, Fig. 3). This effect was observed in each region of interest of the retina compared to the control group. The exception was for the 1 mm isopter in the nasal and inferior quadrants and the 2 mm isopter in the inferior quadrant in the 5% CO₂ group. It appeared that changes seem stronger in peripheral regions (34–53%) than in the center of the retina (30–31%) but this did not reach significance (Fig. 3). Results from whole retina sampling method showed the same significant

Table 1
Effect of hypercapnia on retinal and cerebral blood flow measured by autoradiography and sampling method.

	Control	5% CO ₂	8% CO ₂
<i>Tissue sampling method</i>			
RBF	92 ± 21 (n = 9)	110 ± 13 (n = 4)	121 ± 7* (n = 5)
CBF	97 ± 4 (n = 3)	197 ± 18* (n = 4)	218 ± 3* (n = 4)
<i>Autoradiography</i>			
<i>Whole-mount retina</i>			
Optic nerve head	108 ± 20	140 ± 12*	141 ± 16*
Nasal			
1 mm	119 ± 24	143 ± 5	158 ± 16*
2 mm	102 ± 18	131 ± 10*	145 ± 18**
3 mm	84 ± 15‡	112 ± 14*	131 ± 16**
Temporal			
1 mm	119 ± 20	149 ± 15*	158 ± 19**
2 mm	109 ± 18	137 ± 7**	142 ± 20*
3 mm	86 ± 21	117 ± 12*	132 ± 22**
Superior			
1 mm	113 ± 21	148 ± 8*	157 ± 16**
2 mm	98 ± 16	132 ± 7**	145 ± 14**
3 mm	82 ± 17‡	111 ± 14*	135 ± 18**
Inferior			
1 mm	122 ± 22	144 ± 11	158 ± 15
2 mm	109 ± 20	131 ± 16	142 ± 16*
3 mm	86 ± 18	114 ± 14*	119 ± 16**
<i>Brain sections</i>			
Cingulate Cx	120 ± 22	156 ± 30	237 ± 56*
Frontal Cx	127 ± 12	166 ± 32	239 ± 68*
Parietal Cx	113 ± 23	138 ± 24	222 ± 48*
Occipital Cx	100 ± 12	128 ± 18	180 ± 58*
Striatum	108 ± 12	138 ± 28	189 ± 52*
Hippocampus	70 ± 10	106 ± 20*	168 ± 44*
Dorsal geniculate nucleus	112 ± 22	167 ± 31*	259 ± 55*
Superior colliculus	112 ± 19	147 ± 16*	229 ± 60*

All values are means ± SD and are expressed in ml/100 g/min. For brain sections autoradiography values, the control group was consisted of $n = 6$ animals and both hypercapnic groups were consisted of $n = 4$ animals.

* $p < 0.05$, ** $p < 0.01$ compared with control group. † $p < 0.05$, ‡ $p < 0.01$ isopter 3 mm compared with optic nerve head.

Table 2
Regional measurement of retinal blood flow using the sampling method.

	Tissue sampling (n = 3)	Autoradiography (n = 9)
<i>Isopter</i>		
Optic nerve head	138 ± 18	108 ± 20
1 mm	124 ± 27	119 ± 24
2 mm	114 ± 8	102 ± 18
3 mm	89 ± 13 ^a	84 ± 15 ^a

All values are means ± SD and are expressed in ml/100 g/min.

^a $p < 0.05$ isopter 3 mm compared with optic nerve head.

increase (33%) of RBF values in the 8% CO₂ group compared to control group (92 ± 21 vs. 121 ± 7 ml/100 g/min, $p = 0.019$, Fig. 3, Table 1).

Hypercapnia also induced a robust increase in blood supply in the brain. Increases in CBF induced by hypercapnia were seen in all regions measured by autoradiography and reached about a two-fold increase (Fig. 4, Table 1) in the 8% CO₂ group compared to control. The 5% CO₂ group displayed a significant increase of CBF in the hippocampus (53%, $p = 0.01$), dorsal geniculate nucleus (49%, $p = 0.019$) and superior colliculus (31%, $p = 0.038$) compared to control group, but was not statistically different in cortex and striatum (Fig. 4, Table 1). CBF increases measured by the sampling method were also statistically significant for both hypercapnic groups compared to control group ($p = 0.034$). The blood flow changes induced by hypercapnia were lower in the retina (24–53%) than the brain (22–142%, Figs. 3,4, Table 1, $p = 0.016$).

4. Discussion

This study used an autoradiographic method for the simultaneous quantification of RBF and CBF in non-anesthetised rats. The use of the diffusible tracer [¹⁴C]-IMP provided quantitative measurements of RBF in discrete regions of the retina ranging from the central to peripheral retina. This technique was sensitive enough to quantify differential RBF changes related to two different hypercapnia regimens. Moreover, it allowed for the comparison of blood flow values of the retina to those of the brain.

4.1. Quantitative and regional measurement of retinal blood flow with [¹⁴C]-IMP

The autoradiographic investigation of RBF using [¹⁴C]-IMP described here provided a high resolution quantitative cartography of RBF. Blood tissue perfusion was higher in the central as compared to peripheral retina with autoradiography and sampling method by

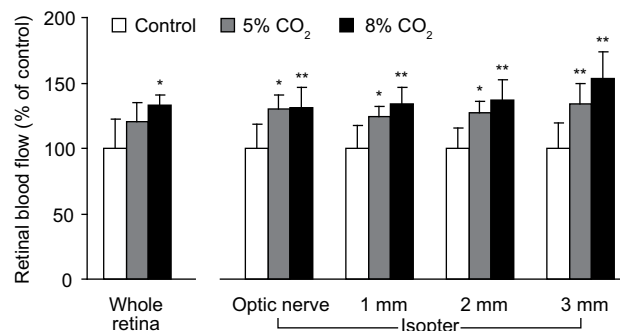


Fig. 3. Percent change (versus control) of the retinal blood flow during hypercapnia. The retinal blood flow was measured on whole retina by sampling method (left panel) or on each isopter by autoradiography (right panel). The retinal blood flow was significantly increased in both hypercapnic groups (5% CO₂ and 8% CO₂) compared to control group at each isopter. * $p < 0.05$ and ** $p < 0.01$, significantly different from control group.

isopters, as seen in monkey (Alm and Bill, 1973). The RBF values were within the same range as reported in other studies using iodoantipyrine as a tracer (O'Brien et al., 1997), but slightly larger than those obtained using microsphere method (Ido et al., 2004; Wang et al., 2007) and smaller than those obtained using hydrogen clearance (Cringle et al., 1993), magnetic resonance imaging (Li et al., 2008) or perfusion by butanol (Puchowicz et al., 2004). Fluctuations in RBF values according to the technique used could result from the use of anesthetics or invasive procedures that might alter the systemic and retinal (Li et al., 2008) blood flow. An advantage of the present technique is the homeostatic preservation of the eye and the cardiovascular system, as well as the vigilant state of the animals. Nevertheless, restraint stress of the animal and acute ischemic tissue injury caused by cannulation of femoral artery and vein could have a slight influence on physiological parameters such as heart rate (Yoshimoto et al., 2008). The dual vascular supply of the retina from central retinal artery and choroid is a puzzling issue for assessing RBF. In the present technique we cannot exclude that a fraction of [¹⁴C]-IMP entrapped in the isolated retina could have diffused from the choroidal circulation through the pigmented epithelium. However, blood flow values would have been much more elevated in that case since choroid blood flow is known to be 10 times higher than RBF (Alm and Bill, 1973; Wang et al., 2007). The conformity of the present measured RBF values with previous studies supports an absence of a significant contamination from choroidal circulation, which is an advantage of the use of [¹⁴C]-IMP over [¹⁴C]-iodoantipyrine (Sossi and Anderson, 1983; Quigley et al., 1985; McFadzean et al., 1989; O'Brien et al.,

Table 3
Effect of hypercapnia on the physiological parameters monitored in the conscious rats after 2 h of recovery from anesthesia and prior to the injection of [¹⁴C]-IMP.

	Control group (n = 9)	5% CO ₂ group (n = 4)		8% CO ₂ group (n = 5)	
		Baseline	During	Baseline	During
Body temperature (°C)	37.4 ± 0.3	38.1 ± 0.3	38.3 ± 0.4	37.9 ± 0.6	37.9 ± 1.0
Blood pressure					
systolic (mmHg)	132 ± 12	130 ± 6	138 ± 3	137 ± 10	138 ± 3
diastolic (mmHg)	104 ± 13	108 ± 7	105 ± 2	110 ± 5	105 ± 2
mean (mmHg)	113 ± 13	115 ± 6	116 ± 5	119 ± 6	116 ± 2
Heart Rate (Beats/min)	500 ± 53	449 ± 20	435 ± 12	461 ± 48	515 ± 83
Arterial pH	7.45 ± 0.01	7.45 ± 0.01	7.27 ± 0.02*	7.45 ± 0.01	7.07 ± 0.04**
Arterial pO ₂ (mmHg)	85.8 ± 3.6	86.8 ± 4.3	106.8 ± 9.0*	85.8 ± 5.2	103.2 ± 7.3*
Arterial pCO ₂ (mmHg)	37.8 ± 1.8	35.1 ± 2.2	57.6 ± 3.4*	35.6 ± 1.4	103.9 ± 16.1**
Arterial HCO ₃ (mmol/L)	26.3 ± 1.3	24.2 ± 1.2	26.3 ± 0.4*	24.8 ± 0.8	29.9 ± 1.3**
Hematocrit (% PVC)	40.7 ± 3.4	37.0 ± 2.8	37.8 ± 3.2	40.0 ± 1.6	43.0 ± 0.7**

Values are means ± SD. pO₂, pCO₂, partial gas pressure of oxygen and carbon dioxide, respectively; HCO₃, bicarbonate; *Baseline*, measure made before the induction of hypercapnia; *During*, measure made 5 min after induction of hypercapnia.

* $p < 0.05$, ** $p < 0.01$ compared with pre-hypercapnic values.

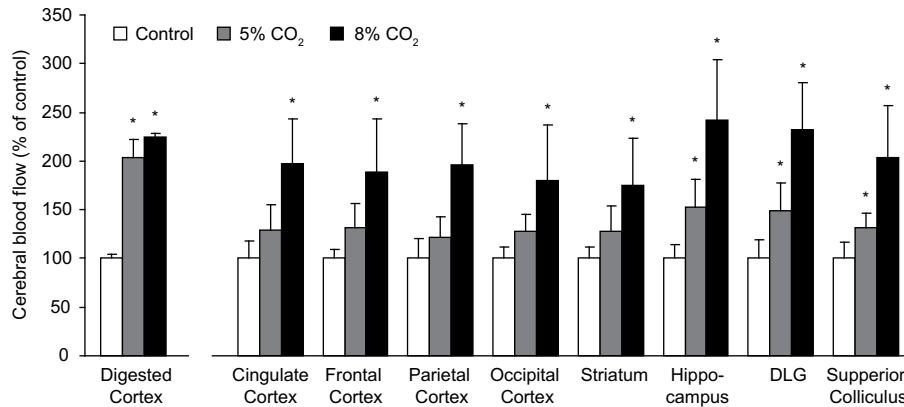


Fig. 4. Percent change (versus control) of the cerebral blood flow during hypercapnia. The cerebral blood flow was measured on a piece of frontal cortex by the sampling method (left panel) or in different brain regions by autoradiography (right panel). Cerebral blood flow was significantly increased in the hippocampus, DLG and superior colliculus of the 5% CO₂ group and in every region measured for the 8% CO₂ group compared to control group. * $p < 0.05$.

1997). The strong post-mortem diffusion of iodoantipyrine requires an immediate freezing of the tissue after the sacrifice of the animal, limiting the study of RBF to cross-sections of the eye globe. On those autoradiograms, the apposition of the choroid to the retina makes it difficult to differentiate the RBF from the choroidal blood flow (Caprioli and Miller, 1988), which is not the case with flat mount retinæ. The main limitation of the autoradiographic technique is that it provides a snapshot measurement of RBF unlike microsphere technique which permits a small number of consecutive measurements to be made in one animal (Alm and Bill, 1973; Wang et al., 2008).

Results showed that hypercapnia significantly increased the retinal blood flow as reported in a previous study using the microsphere method in rats (Wang et al., 2008). The technique showed a good sensitivity since the changes measured were proportional to the pCO₂ of the animals. This validates the ability of the method to assess graduated variations of RBF. There was a good correspondence in percentage of change in blood flow in hypercapnic conditions using the sampling or autoradiography method, indicating that autoradiographic RBF measurements allowed valid intergroup comparisons of retinal regions.

4.2. Comparison of retinal blood flow with cerebral blood flow

Our findings demonstrated that under normocapnic conditions, retinal perfusion was similar to blood flow in cerebral cortex, i.e. in the range of 95 ml/100 g/min. These results agree with previous studies using the microsphere method which showed that RBF was similar to CBF in rats (Tilton et al., 1988, 1999) and monkeys (Alm and Bill, 1973). Results from the n-[¹⁴C]Butanol method suggested RBF is lower than CBF in rats (Puchowicz et al., 2004) which may be caused by post-mortem diffusion of the tracer. Evaluation of blood flow with blood-oxygenation level dependent (BOLD) functional magnetic resonance imaging indicated that RBF was five-fold greater than CBF in rats (Sicard and Duong, 2005; Li et al., 2008, 2009). However the resolution level might not have been adequate to discriminate retinal from choroidal blood flow. The current technique appears to provide an advantage over other techniques in terms of comparison of blood perfusion in different organs. This is important to evaluate the impact of a treatment on different vascular beds.

Our results showed a higher reactivity of blood flow in the brain than in the retina during CO₂ inhalation. Blood flow in the brain reached up to 142% augmentation in the 8% CO₂ group while mean RBF was increased up to 53%. These results suggest that the cerebral vascular bed might be more reactive to pCO₂ changes than the

retina. Such findings have been observed in a study using microsphere method in piglets (Stiris et al., 1989).

5. Conclusion

In summary, we demonstrated that RBF can be quantitatively and regionally measured with [¹⁴C]-IMP in rats. This offers a beneficial opportunity for ophthalmology research since most ocular diseases are characterized by discrete and circumscribed changes in blood flow. The possibility to compare quantitative data of RBF in different groups is essential for the evaluation of pharmaceutical treatments or to detect the subtle changes of blood flow in the retina of ocular diseases models.

Acknowledgements

The authors would like to thank Florence Dotigny for her technical assistance, Denis Latendresse for his graphical help, Mark Burke and Pierre Lacombe (Université Paris VII) for careful reading of the manuscript and helpful discussion. This study was supported by CNIB Baker New Researcher Fund, Canadian Foundation for Innovation (E.V.) and the Vision Research Network (FRSQ). MP is a recipient of the graduate student scholarship from the Foundation Fighting Blindness. EV received a Chercheur-Boursier salary support from Fonds de Recherche en Santé du Québec (FRSQ).

References

- Alm, A., Bill, A., 1973. Ocular and optic nerve blood flow at normal and increased intraocular pressures in monkeys (Macaca irus): a study with radioactively labelled microspheres including flow determinations in brain and some other tissues. *Exp. Eye Res.* 15, 15–29.
- Alm, A., Lambrou, G.N., Maepea, O., Nilsson, S.F., Percicot, C., 1997. Ocular blood flow in experimental glaucoma: a study in cynomolgus monkeys. *Ophthalmologica* 211, 178–182.
- Atmaca, L.S., Batioglu, F., Atmaca, P., 1996. Evaluation of choroidal neovascularization in age-related macular degeneration with fluorescein and indocyanine green videoangiography. *Ophthalmologica* 210, 148–151.
- Bryan Jr., R.M., Myers, C.L., Page, R.B., 1988. Regional neurohypophysial and hypothalamic blood flow in rats during hypercapnia. *Am. J. Physiol.* 255, R295–R302.
- Caprioli, J., Miller, J.M., 1988. Measurement of optic nerve blood flow with iodoantipyrine: limitations caused by diffusion from the choroid. *Exp. Eye Res.* 47, 641–652.
- Chauhan, B.C., Yu, P.K., Cringle, S.J., Yu, D.Y., 2006. Confocal scanning laser Doppler flowmetry in the rat retina: origin of flow signals and dependence on scan depth. *Arch. Ophthalmol.* 124, 397–402.
- Chemtob, S., Beharry, K., Rex, J., Chatterjee, T., Varma, D.R., Aranda, J.V., 1991. Ibuprofen enhances retinal and choroidal blood flow autoregulation in newborn piglets. *Invest. Ophthalmol. Vis. Sci.*, 1799–1807.

- Clermont, A.C., Britts, M., Shiba, T., McGovern, T., King, G.L., Bursell, S.E., 1994. Normalization of retinal blood flow in diabetic rats with primary intervention using insulin pumps. *Invest. Ophthalmol. Vis. Sci.* 35, 981–990.
- Cringle, S.J., Yu, D.Y., Alder, V.A., Su, E.N., 1993. Retinal blood flow by hydrogen clearance polarography in the streptozotocin-induced diabetic rat. *Invest. Ophthalmol. Vis. Sci.* 34, 1716–1721.
- Dauphin, F., Lacombe, P., Sercombe, R., Hamel, E., Seylaz, J., 1991. Hypercapnia and stimulation of the substantia innominata increase rat frontal cortical blood flow by different cholinergic mechanisms. *Brain Res.* 553, 75–83.
- Duong, T.Q., Pardue, M.T., Thule, P.M., Olson, D.E., Cheng, H., Nair, G., Li, Y., Kim, M., Zhang, X., Shen, Q., 2008. Layer-specific anatomical, physiological and functional MRI of the retina. *NMR Biomed.* 21, 978–996.
- Fujimoto, J.G., Brezinski, M.E., Tearney, G.J., Boppart, S.A., Bouma, B., Hee, M.R., Southern, J.F., Swanson, E.A., 1995. Optical biopsy and imaging using optical coherence tomography. *Nat. Med.* 1, 970–972.
- Glazer, L.C., 1988. Methods for determination of optic nerve blood flow. *Yale J. Biol. Med.* 61, 51–60.
- Greenberg, J.H., Sohn, N.W., Hand, P.J., 1999. Nitric oxide and the cerebral-blood-flow response to somatosensory activation following deafferentation. *Exp. Brain Res.* 129, 541–550.
- Grunwald, J.E., Riva, C.E., Brucker, A.J., Sinclair, S.H., Petrig, B.L., 1984. Altered retinal vascular response to 100% oxygen breathing in diabetes mellitus. *Ophthalmology* 91, 1447–1452.
- Ido, Y., Chang, K., Williamson, J.R., 2004. NADH augments blood flow in physiologically activated retina and visual cortex. *Proc. Natl. Acad. Sci. U.S.A.* 101, 653–658.
- Kunisaki, M., Bursell, S.E., Umeda, F., Nawata, H., King, G.L., 1998. Prevention of diabetes-induced abnormal retinal blood flow by treatment with d-alpha-tocopherol. *Biofactors* 7, 55–67.
- Langham, M.E., Grebe, R., Hopkins, S., Marcus, S., Sebag, M., 1991. Choroidal blood flow in diabetic retinopathy. *Exp. Eye Res.* 52, 167–173.
- Lear, J.L., Ackermann, R.F., Kameyama, M., Kuhl, D.E., 1982. Evaluation of [123I]isopropylidoamphetamine as a tracer for local cerebral blood flow using direct autoradiographic comparison. *J. Cereb. Blood Flow Metab.* 2, 179–185.
- Li, Y., Cheng, H., Duong, T.Q., 2008. Blood-flow magnetic resonance imaging of the retina. *Neuroimage* 39, 1744–1751.
- Li, Y., Cheng, H., Shen, Q., Kim, M., Thule, P.M., Olson, D.E., Pardue, M.T., Duong, T.Q., 2009. Blood-flow magnetic resonance imaging of retinal degeneration. *Invest. Ophthalmol. Vis. Sci.* 50, 1824–1830.
- McFadzean, R.M., Graham, D.I., Lee, W.R., Mendelow, A.D., 1989. Ocular blood flow in unilateral carotid stenosis and hypotension. *Invest. Ophthalmol. Vis. Sci.* 30, 487–490.
- Mori, A., Saito, M., Sakamoto, K., Nakahara, T., Ishii, K., 2007. Intravenously administered vasodilatory prostaglandins increase retinal and choroidal blood flow in rats. *J. Pharmacol. Sci.* 103, 103–112.
- O'Brien, C., Kelly, P.A., Ritchie, I.M., 1997. Effect of chronic inhibition of nitric oxide synthase on ocular blood flow and glucose metabolism in the rat. *Br. J. Ophthalmol.* 81, 68–71.
- Puchowicz, M.A., Xu, K., Magness, D., Miller, C., Lust, W.D., Kern, T.S., LaManna, J.C., 2004. Comparison of glucose influx and blood flow in retina and brain of diabetic rats. *J. Cereb. Blood Flow Metab.* 24, 449–457.
- Quigley, H.A., Hohman, R.M., Sanchez, R., Addicks, E.M., 1985. Optic nerve head blood flow in chronic experimental glaucoma. *Arch. Ophthalmol.* 103, 956–962.
- Sakurada, O., Kennedy, C., Jehle, J., Brown, J.D., Carbin, G.L., Sokoloff, L., 1978. Measurement of local cerebral blood flow with iodo [14C] antipyrine. *Am. J. Physiol.* 234, H59–H66.
- Sicard, K.M., Duong, T.Q., 2005. Effects of hypoxia, hyperoxia, and hypercapnia on baseline and stimulus-evoked BOLD, CBF, and CMRO2 in spontaneously breathing animals. *Neuroimage* 25, 850–858.
- Sossi, N., Anderson, D.R., 1983. Effect of elevated intraocular pressure on blood flow. Occurrence in cat optic nerve head studied with iodoantipyrine I 125. *Arch. Ophthalmol.* 101, 98–101.
- Stiris, T., Odden, J.P., Hansen, T.W., Hall, C., Bratlid, D., 1989. The effect of arterial PCO2-variations on ocular and cerebral blood flow in the newborn piglet. *Pediatr. Res.* 25, 205–208.
- Temma, T., Magata, Y., Mukai, T., Kitano, H., Konishi, J., Saji, H., 2004. Availability of N-isopropyl-p-[125I]iodoamphetamine (IMP) as a practical cerebral blood flow (CBF) indicator in rats. *Nucl. Med. Biol.* 31, 811–814.
- Tilton, R.G., Chang, K., Weigel, C., Eades, D., Sherman, W.R., Kilo, C., Williamson, J.R., 1988. Increased ocular blood flow and 125I-albumin permeation in galactose-fed rats: inhibition by sorbinil. *Invest. Ophthalmol. Vis. Sci.* 29, 861–868.
- Tilton, R.G., Chang, K.C., Lejeune, W.S., Stephan, C.C., Brock, T.A., Williamson, J.R., 1999. Role for nitric oxide in the hyperpermeability and hemodynamic changes induced by intravenous VEGF. *Invest. Ophthalmol. Vis. Sci.* 40, 689–696.
- Tsujikawa, A., Kiryu, J., Nonaka, A., Yamashiro, K., Ogura, Y., Honda, Y., 2000. Reproducibility of scanning laser Doppler flowmetry in the rat retina and optic nervehead. *Jpn. J. Ophthalmol.* 44, 257–262.
- Vaucher, E., Borredon, J., Bonvento, G., Seylaz, J., Lacombe, P., 1997. Autoradiographic evidence for flow-metabolism uncoupling during stimulation of the nucleus basalis of Meynert in the conscious rat. *J. Cereb. Blood Flow Metab.* 17, 686–694.
- Wang, L., Fortune, B., Cull, G., McElwain, K.M., Cioffi, G.A., 2007. Microspheres method for ocular blood flow measurement in rats: size and dose optimization. *Exp. Eye Res.* 84, 108–117.
- Wang, L., Grant, C., Fortune, B., Cioffi, G.A., 2008. Retinal and choroidal vasoreactivity to altered PaCO2 in rat measured with a modified microsphere technique. *Exp. Eye Res.* 86, 908–913.
- Yoshimoto, M., Wehrwein, E.A., Novotny, M., Swain, G.M., Kreulen, D.L., Osborn, J.W., 2008. Effect of stellate ganglionectomy on basal cardiovascular function and responses to beta1-adrenoceptor blockade in the rat. *Am. J. Physiol. Heart Circ. Physiol.* 295, H2447–H2454.
- Yu, D.Y., Townsend, R., Cringle, S.J., Chauhan, B.C., Morgan, W.H., 2005. Improved interpretation of flow maps obtained by scanning laser Doppler flowmetry using a rat model of retinal artery occlusion. *Invest. Ophthalmol. Vis. Sci.* 46, 166–174.